SCIENTIFIC REPORTS

OPEN

SUBJECT AREAS:
COORDINATION CHEMISTRY
FUEL CELLS

Received
10 March 2014

Accepted
14 May 2014

Published
30 May 2014

Correspondence and requests for materials should be addressed to Y.-Q.L. (yqlan@njnu.edu.cn) or Z.H.D. (daizhihuii@njnu.edu.cn)

Heteroatoms ternary-doped porous carbons derived from MOFs as metal-free electrocatalysts for oxygen reduction reaction

Ji-Sen Li[1,2], Shun-Li Li[1], Yu-Jia Tang[1], Kui Li[1], Lei Zhou[1], Ning Kong[1], Ya-Qian Lan[1], Jian-Chun Bao[1] & Zhi-Hui Dai[1]

[1]Jiangsu Key Laboratory of Biofunctional Materials, College of Chemistry and Materials Science, Nanjing Normal University, Nanjing 210023, P. R. China, [2]Department of Chemistry and Chemical Engineering, Jining University, Qufu 273155, P. R. China.

The nitrogen (N), phosphorus (P) and sulphur (S) ternary-doped metal-free porous carbon materials have been successfully synthesized using MOFs as templates (denoted as NPS-C-MOF-5) for oxygen reduction reaction (ORR) for the first time. The influences of porous carbons from carbonizing different MOFs and carbonization temperature on ORR have been systematically investigated. Due to the synergistic effect of N, P and S ternary-doping, the NPS-C-MOF-5 catalyst shows a higher onset potential as a metal-free electrocatalyst for ORR among the currently reported metal-free electrocatalysts, very close to the commercial Pt-C catalyst. In particular, the kinetic limiting current density of NPS-C-MOF-5 catalyst at −0.6 V is up to approximate −11.6 mA cm^{-2}, which is 1.2 times higher than that of the commercial Pt-C catalyst. Furthermore, the outstanding methanol tolerance and excellent long-term stability of NPS-C-MOF-5 are superior to those of the commercial Pt-C catalyst for ORR in alkaline media.

The sluggish kinetics of oxygen reduction reaction (ORR) at fuel cells (FCs) cathode seriously hinder the overall development of efficient energy storage and conversion devices[1,2], so catalysts must be used to enhance the efficiency of fuel cells. Currently, the platinum[3–5] (Pt) and Pt-based[6–10] catalysts are common for ORR. However, there are some vital problems still plaguing Pt-based catalysts such as high cost, limited quantity available, poor stability and susceptibility to methanol crossover. Thus, this is a crucial issue in the development and application of FCs, namely, replacing precious and nondurable Pt-based catalysts with cheap and highly efficient materials for ORR.

Recently, carbon materials as metal-free catalysts for ORR have attracted considerable attention, due to low cost, long-term stability and excellent methanol tolerance. In particular, heteroatom doped (e.g., B[11–13], N[14–19], P[20–23] and S[24–28]) carbon materials have been the most active research topics because more active sites derived from heteroatom-doping are favorable for enhancing ORR activities. On the other hand, metal-organic frameworks (MOFs), characteristic of a novel class of porous materials, have drawn particular interest during the past decades[29–31]. Xu's group first reported MOF-templated porous carbon materials using MOF-5 as a template[32]. Subsequently, there have been more reports on porous carbon materials obtained from MOF templates for different applications[33,34]. Nevertheless, only a limited number of MOF-templated carbons as electrocatalysts for ORR have been investigated[35–39]. Unfortunately, trace metals are still maintained in the resulting MOF-templated carbon materials. Additionally, very scarce reports concern about multi-heteroatoms doping carbon materials for ORR to date[40,41]. To the best of our knowledge, the ternary-doped (N, P and S) metal-free carbon materials fabricated by post-synthesis modification of MOFs for ORR remain largely unexplored so far. Taking into account the tremendous potential of ternary-doped metal-free carbon materials, it is a significant and challengeable task to synthesize ternary-doped metal-free porous carbon materials for ORR, especially using MOFs as a template.

Herein, we have first fabricated N, P and S ternary-doped metal-free porous carbon materials using MOF-5 as a template and dicyandiamid (DCDA), triarylphosphine (TPP) and dimethyl sulfoxide (DMSO) as N, P and S precursors (designated as NPS-C-MOF-5) for the ORR. The influences of porous carbons from carbonizing different MOFs and carbonization temperature on ORR were systematically investigated. Compared with the

other carbon materials, the NPS-C-MOF-5 catalyst shows higher electrocatalytic activity, outstanding methanol tolerance and excellent long-term stability due to the synergistic effect of N, P and S ternary-doping. On the other hand, the doped samples with different active sites and increasing percentage of mesopores may be major causes of different ORR activities.

Results

The synthetic process for preparing NPS-C-MOF-5 as a metal-free catalyst for the ORR was illustrated in Figure 1. Briefly, MOF-5 was synthesized according to the reported method[42] and chosen as a template. DCDA, TPP and DMSO were chosen as N, P and S precursors, respectively. The doping process was carried out by soaking the dried MOF-5 in methanol solution in the presence of DCDA, TPP and DMSO and then carbonized at 900°C in ultrapure N_2. The obtained materials were washed with dilute hydrochloric acid solution and distilled water, respectively. For comparison, the undoped, N-doped, NS or NP co-doped porous carbons (defined as C-MOF-5, N-C-MOF-5, NS-C-MOF-5 or NP-C-MOF-5) were also treated under similar conditions, respectively.

The powder X-Ray diffraction (PXRD) pattern of MOF-5 crystals is most identical with the simulated and the transparent cubic crystals reveal the high crystallinity of the products (Figure S1). As shown in Figure S2, the PXRD profiles for the obtained carbon materials with two broad peaks at around 25 and 44° prove their amorphous nature. The absence of diffraction peaks of Zn impurities indicates the complete removal of carbon-reduced Zn metal from the resulted porous carbon materials[32]. Transmission electron microscopy (TEM) (Figure 2a and Figure S3) and scanning electron microscope (SEM) (Figure S4) images suggest the porous nature of the resulting carbon materials. On the other hand, N, P and S doped into the resulted carbon materials could be directly visualized from the energy dispersive X-ray spectroscopy (EDS) (Figures 2b and S5) and the corresponding elemental mapping of NPS-C-MOF-5 (Figures 2c–h).

In order to further investigate the structural information, Raman D- and G-band intensities were used to characterize the carbon materials, particularly analyze the crystallization degree of graphitic carbon. Two peaks at about 1350 and 1598 cm^{-1} correspond to the D and G band, respectively[26,37]. The former peak is attributed to an A_{1g} vibration mode of carbon atoms with dangling bonds in plane terminations of disorder graphite. The latter peak is associated with the vibration of all sp^2 hybridized carbon atoms of the carbon layer. Remarkably, it was found that the I_D/I_G of NPS-C-MOF-5 was higher than that of C-MOF-5, N-C-MOF-5, NS-C-MOF-5 and NP-C-MOF-5 (Figure S6). The result shows that more defects and active sites are developed which are ascribed to the N, P and S ternary-doping, which are beneficial for the ORR.

The chemical composition of NPS-C-MOF-5 was investigated by X-ray photoelectron spectroscopy (XPS). Figure 3a shows C_{1s}, N_{1s}, O_{1s}, S_{2s}, S_{2p} and P_{2p} peaks for NPS-C-MOF-5, respectively, which also suggests that N, P and S were successfully doped into NPS-C-MOF-5. The O peak is assigned to the physicochemically adsorbed oxygen[20], which is advantageous for ORR. The high resolution XPS N_{1s} spectrum (Figure 3b) can be divided into three peaks, corresponding to graphitic N (~401.2 eV), pyrrolic N (~399.8 eV) and pyridinic N (~398.6 eV)[37], respectively. Compared to pyrrolic nitrogen, the graphitic and pyridinic N are the main components indicating the highest ORR performance[43]. From Figure 3c, it can be seen that the P_{2p} peak at approximate 132.0 eV is attributed to the P-C bonding[21]. In addition, the $S_{2p\ 3/2}$ (163.8 eV) and $S_{2p\ 1/2}$ (164.8 eV) peaks are ascribed to sulphide groups (-C-S-C) (Figure 2d)[44]. The -C-SO_x-C peak (168.5 eV) is also observed in Figure 3d, which is chemically inactive for ORR[25]. For comparison, the other samples were evaluated by XPS measurements (Figure S7). To the best of our knowledge, this is the first report of N, P and S ternary-doped porous carbon materials using MOFs as a template.

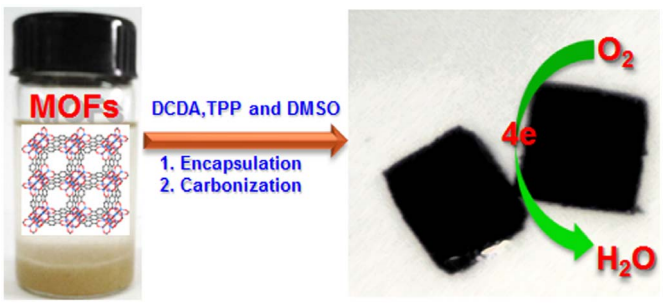

Figure 1 | Schematic illustration of the synthesis of MOF-templated NPS-C-MOF-5 as a metal-free electrocatalyst for the ORR.

The surface textural characteristics for different samples were estimated by N_2 adsorption-desorption isotherms. From Figure 4a, the hysteresis can be seen between adsorption and desorption branches for these samples, which shows the emerging mesopores[45]. Additionally, the pore-size distributions at low pressure were calculated by density functional theory (DFT) in the micropore region (Figure 4b). On the contrary, the corresponding pore-size distributions at high pressure were assessed by Barret-Joyner-Halenda (BJH) model according the desorption branch (Figure 4c). The detailed data were summarized in Table S1. According to Figure 4 and Table S1, it can be speculated that partial micropores of heteroatom-doped samples could be sintered, further reducing the percentage of micropores and increasing the percentage of mecropores. Compared the other samples, although the surface area of NPS-C-MOF-5 is lower, the mesopore volume percentage of NPS-C-MOF-5 is higher (Table S1).

Discussion

To assess the electrocatalytic properties of these carbon materials, cyclic voltammograms (CVs) were carried out in N_2- or O_2-saturated 0.1 M KOH solution at a scan rate of 100 mV s^{-1}. Clearly, all carbon materials appear obvious peaks in the O_2-saturated solution, compared with unnoticed current observed in the N_2-saturated solution (Figure 5a and Figures S8a–e). Notably, the peak potential of NPS-C-MOF-5 catalyst is more positive than that of the other carbon materials, and is slightly negative compared with the commercial Pt-C catalyst (−0.13 V) (Figure S8f). The cathodic current density of NPS-C-MOF-5 catalyst is much higher than the signal of the commercial Pt-C catalyst. Hence, these results clearly demonstrate that the NPS-C-MOF-5 catalyst is an outstanding catalyst for ORR.

To gain additional insight into ORR with the NPS-C-MOF-5 catalyst, linear sweep voltammograms (LSVs) were performed on a rotating-disk electrode (RDE) at a scan rate of 10 mV s^{-1} and different rotating speeds from 400 to 1600 rpm in O_2-saturated 0.1 M KOH solution; comparative experiments were explored for the other carbon materials. As seen from Figure 5b and Figures S9a–d, the current density was enhanced with increasing rotating rate from 400 to 1600 rpm due to facilitating diffusion of electrolytes. In terms of onset potential (Figure 5c), this is about −0.006 V at 1600 rpm for NPS-C-MOF-5 catalyst, which is more positive than that of the other carbon materials. Notably, the NPS-C-MOF-5 catalyst shows a higher onset potential as a metal-free electrocatalyst for ORR among the currently reported metal-free electrocatalysts (Table S2), very close to the commercial Pt-C catalyst (0.03 V), due to the synergistic effect of N, P and S ternary-doping. Surprisingly, the order of onset potentials (NPS-C-MOF-5 > NP-C-MOF-5 > C-MOF-5 > NS-C-MOF-5 > N-C-MOF-5) is not consistent with the order of BET surface areas for these samples (C-MOF-5 > NP-C-MOF-5 > NS-C-MOF-5 > N-C-MOF-5 > NPS-C-MOF-5). So it implies that BET surface areas are not crucial factors for electrocatalytic activities of these catalysts for the ORR. On the contrary, owing to N, P and S

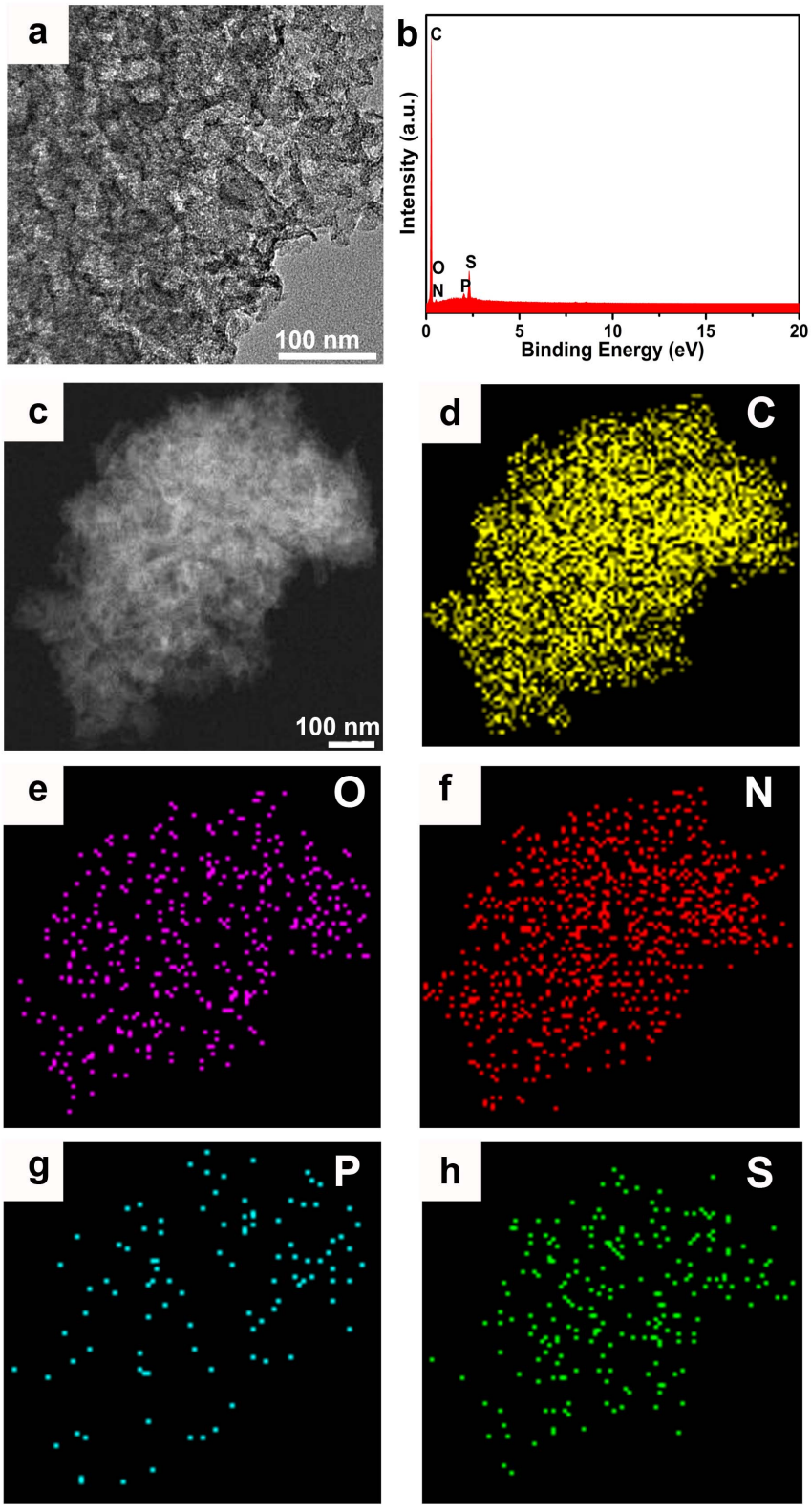

Figure 2 | **(a) TEM, (b) EDS and (c) STEM images of NPS-C-MOF-5, (d–h) the corresponding C-, O-, N-, P- and S- elemental mappings, respectively.**

ternary-doping, the doped samples with different active sites and increasing percentage of mesopores may be major causes of different ORR activities. All of these results are in agreement with those of TEM, SEM and Raman spectra results.

On further study into ORR processes of theses carbon materials, RDE voltammetry measurements were then performed with different rotating rates from 400 to 1600 rpm. The corresponding Koutecky-Levich (K-L) plots over the electrode potential range from −0.4 to −0.9 V show good linearity, implying first-order reaction kinetics toward O_2 reduction within the potential range (Figure S10). From Figure 5d, it can be seen that the NPS-C-MOF-5 catalyst exhibits clearly higher current density than that of the other carbon materials

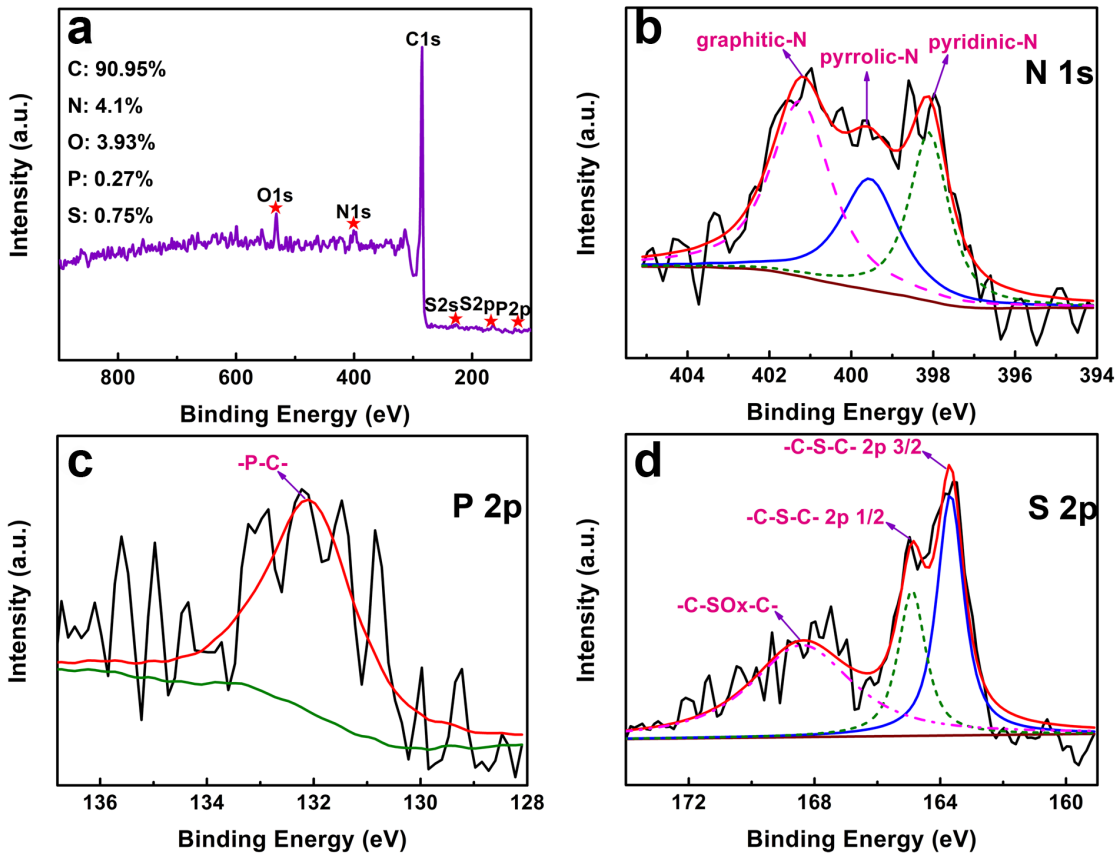

Figure 3 | (a) XPS survey spectrum and high resolution XPS spectra of (b) N 1s, (c) P 2p and (d) S 2p of NPS-C-MOF-5, respectively.

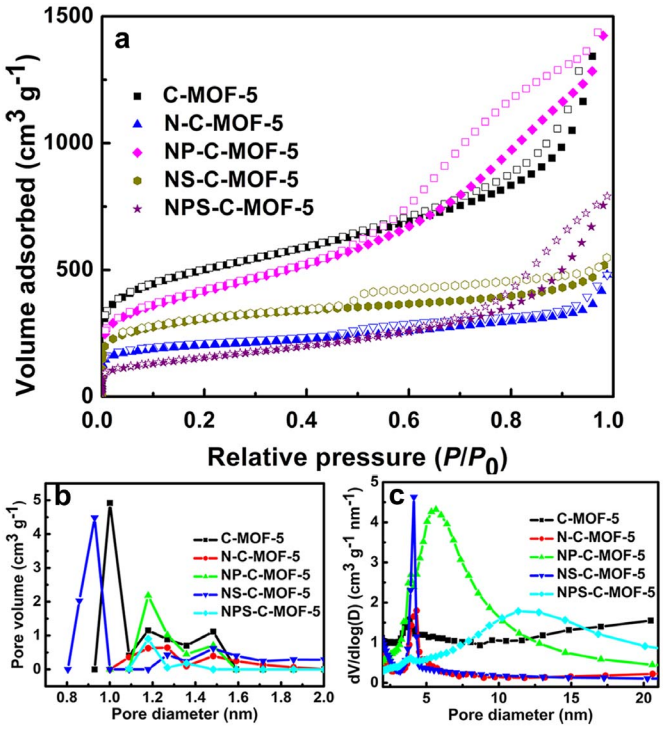

Figure 4 | (a) N_2 adsorption-desorption isotherms, (b) microporous size distributions by DFT model and (c) mesoporous size distributions of different samples by BJH model.

and commercial Pt-C catalyst. This is further demonstration of the predominant ORR electrocatalytic capability on the ternary-doped carbon materials as compared to other corresponding carbon materials. The electron-transfer numbers (n) can be calculated according to the K-L equation (Figure 5e)[25], which is shown in experiment section. The n values of NPS-C-MOF-5 catalyst calculated from the slopes of K-L plots are 3.5–3.9 from −0.4 to −0.9 V, suggesting a favorable 4e pathway of the ORR, with water as the main product. In comparison with NPS-C-MOF-5, the n values of other carbon materials are in the range of 2.8 to 3.7 from −0.4 to −0.9 V (Figure S10). The kinetic limiting current density (J_k) of NPS-C-MOF-5 catalyst is greater than that of the other samples (Figure 5f). In particular, the J_k value of NPS-C-MOF-5 catalyst at −0.6 V is up to approximate −11.6 mA cm^{-2}, which is 1.2 times higher than that of the commercial Pt-C catalyst (−9.7 mA cm^{-2}, −0.6 V). As mentioned above, these results sufficiently reveal that NPS-C-MOF-5 is a potential alternative metal-free catalyst with high catalytic activity for ORR due to the synergetic effect of N, P and S ternary-doping. As far as we know, this work represents the first example of highly effective metal-free porous carbon materials ternary-doped by N, P and S using MOFs as a template for ORR so far.

Tolerance to methanol crossover and durability of electrocatalysts for ORR are critical parameters for the practical applications to FCs. As shown in Figure 6a, there was no noticed change in CV curves for the NPS-C-MOF-5 electrode when methanol was added into O_2-saturated 0.1 M KOH solution. For comparison, the ORR signal of the commercial Pt-C electrode disappeared at about −0.13 V in CVs coupled with one new peak characteristic of methanol reduction/oxidation attributed to methanol poisoning the cathode catalyst (Figure S11). This indicates that the NPS-C-MOF-5 catalyst has an excellent ability for avoiding methanol crossover, even superior to that of the commercial Pt-C catalyst. Figure 6b indicates the resulted current-time (i-t) chronoamperometric response for NPS-C-MOF-5

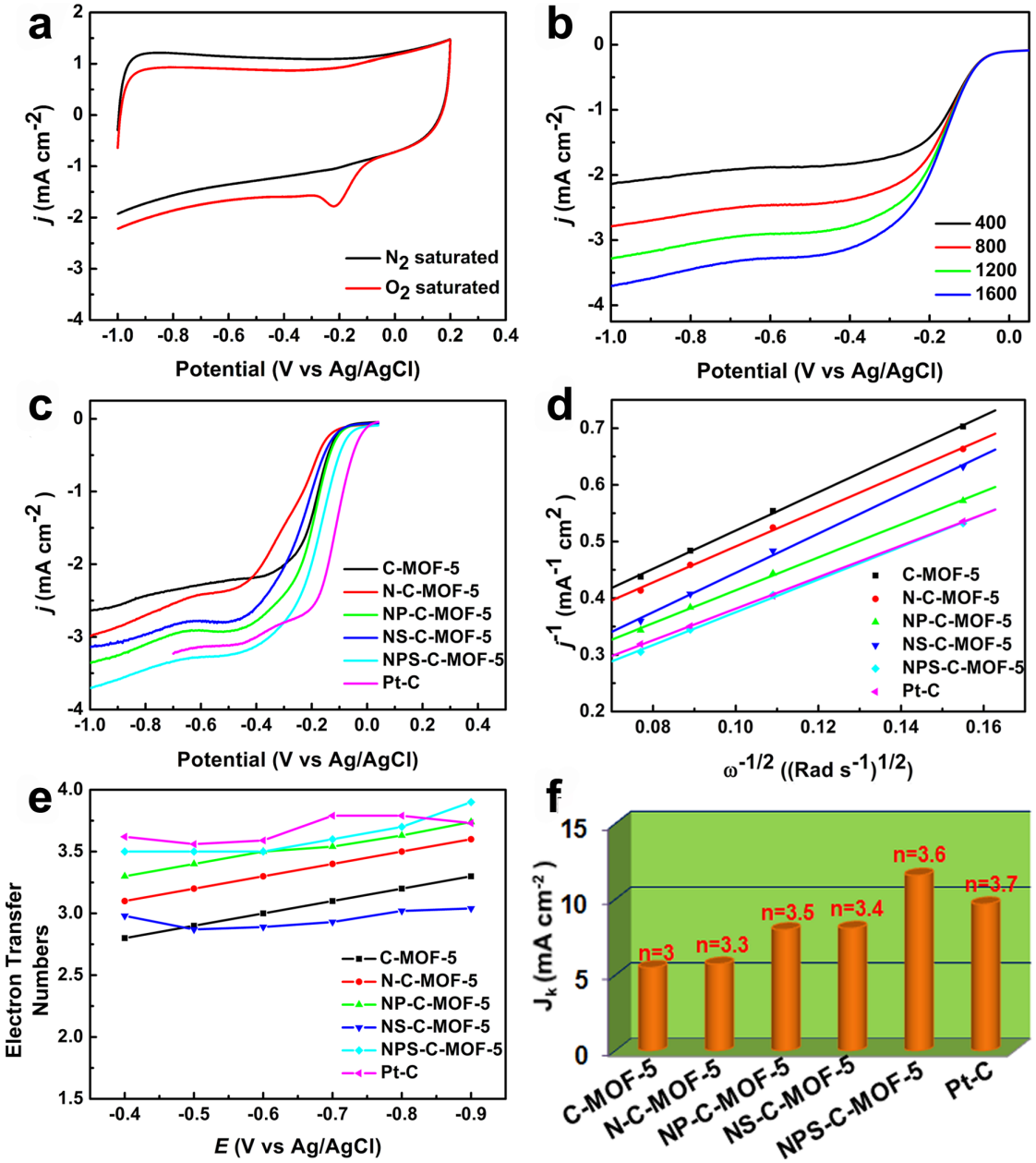

Figure 5 | Electrocatalytic performances of different samples. (a) CVs of NPS-C-MOF-5 in N_2- or O_2-saturated 0.1 M KOH solution; (b) LSVs of NPS-C-MOF-5 at various rotation rates; (c) LSVs of different samples at a rotation rate of 1600 rpm; (d) K-L plots of different samples at −0.6 V; (e) Electron-transfer numbers of different samples from −0.4 to −0.9 V; (f) Kinetic limiting current densities of different samples and the corresponding electron-transfer numbers at −0.6 V.

and Pt-C catalysts in 0.1 M KOH with continuous oxygen reduction (20000 s) at −0.4 V (vs. Ag/AgCl). Compared with the 27% loss of current at the commercial Pt-C electrode due to loss of active metal particles[6], 80% of the initial current could be still persisted at the NPS-C-MOF-5 electrode attributed to the strong strength of covalent heteroatom-carbon bond[26]. The remarkably better stability makes NPS-C-MOF-5 catalyst as a feasible candidate for ORR, especially for methanol alkaline FCs.

The excellent electrocatalytic activity of NPS-C-MOF-5 may be based on the following reasons: 1) Generally speaking, the electronegativity of heteroatoms (e.g., N: 3.04, P: 2.19, S: 2.58) is different from that of carbon atoms (C: 2.55). When heteroatoms are doped into a carbon framework, the electroneutrality is broken to explore a higher number of active sites, which facilitate the adsorption of O_2 and significantly enhance the rate of the overall ORR process[17,41]; 2) Because heteroatoms are incorporated into the carbon materials, the changed asymmetric spin density of heteroatoms can effectively weak the O-O bonding to provide more active sites and enhance the ORR activity of carbon materials[26]; 3) The pore structures of carbon materials are changed owing to heteroatoms doping. The production with different active sites and increasing percentage of mesopores have remarkable influences on the corresponding electrocatalytic activities; 4) The electrocatalytic activity of N, P and S ternary-doped carbon material is superior to correspondingly sole or dual co-doped counterparts due to a synergetic effect of N, P and S ternary-doping[26,44].

In order to investigate the influences of porous carbons from carbonizing different MOFs on ORR, MOF-177 and UMCM-1 crystals were synthesized according to the reported method[46], respectively. The powder PXRD profiles and optical micrographs of the two

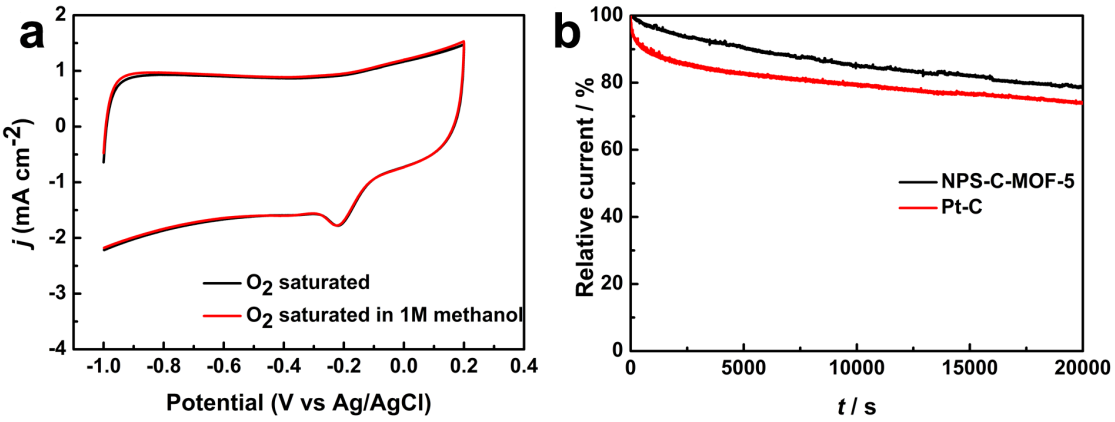

Figure 6 | (a) CVs for the ORR at the NPS-C-MOF-5 electrode in an O_2-saturated 0.1 M KOH solution or an O_2-saturated 0.1 M KOH solution upon addition of methanol; (b) Current-time (i-t) chronoamperometric response of NPS-C-MOF-5 and commercial Pt-C electrodes at −0.4 V in O_2-saturated 0.1 M KOH at a rotation rate of 1600 rpm.

precursors are shown in Figure S12 and Figures 7e–f. The PXRD patterns of the synthesized crystals are in agreement with the peaks of those simulated. After carbonization, the obtained samples were denoted as C-MOF-177 and C-UMCM-1 (Figures 7h–i), which were investigated by SEM (Figure S13), HRTEM (Figure S14), EDS (Figure S15) N_2 adsorption-desorption isotherm (Figure S16), PXRD (Figure S17a) and Raman spectroscopy (Figure S17b), respectively. The textural properties of corresponding samples were summarized in Table S3. The results are similar to that of C-MOF-5. Remarkably, the I_G/I_D value of C-MOF-5 is maximal among the three carbon materials, which further shows the higher degree of graphitization for C-MOF-5 than the other carbon materials.

The electrocatalytic activities of the three porous carbons for the ORR were estimated by CVs and LSVs, respectively. The order of peak potentials of the three porous carbons is found to be C-MOF-5 > C-UMCM-1 > C-MOF-177 (Figure 7j), which agrees with the order of their onset potentials (Figure 7k). From the optical micrographs after carbonization (Figures 7g–i), the original morphologies of crystals are retained in the resulting porous carbons, which prove that the characteristics of porous carbons are related to different MOF structures. We think that different porous carbons can be obtained by carbonizing MOFs with different structures, which may have powerful effect on ORR as highly efficient metal-free electrocatalysts.

In order to further evaluate the influence of carbonization temperature for ORR, carbonization procedures of MOF-5 were carried out at 700, 900 and 1000°C (denoted as C-MOF-5-700, C-MOF-5-900 and C-MOF-5-1000), respectively. The CVs and LSVs were performed to investigate their ORR activities, respectively. Figure S18 shows that C-MOF-5-900 exhibits the most positive peak potential and onset potential for the ORR among the three samples, indicating that C-MOF-5-900 holds the most excellent electrocatalytic activity. Hence, the optimum temperature appeared to be 900°C.

In conclusion, we have successfully synthesized a novel kind of N, P and S ternary-doped metal-free carbon materials using MOF-5 as a template for ORR for the first time. The different structures and compositions of MOFs have an important impact on the electrocatalytic activities of porous carbons for ORR. Meanwhile, the influence of carbonization temperature on ORR was systematically investigated. When heteroatoms are doped into carbon materials, the pore structures of these samples are changed, and then the doped samples with different active sites and increasing percentage of mesopores may be major causes of different ORR activities. In particular, due to the synergistic effect of N, P and S ternary-doping, the NPS-C-MOF-5 catalyst shows a higher onset potential as a metal-free electrocatalyst for ORR among the currently reported metal-free electrocatalysts, very close to the commercial Pt-C catalyst. Additionally, the outstanding methanol tolerance and excellent long-term stability of NPS-C-MOF-5 catalyst are superior to those of the commercial Pt-C catalyst for ORR in alkaline media. The results provide a new avenue for the development of multi-heteroatoms doped carbon materials using MOFs as a template for FC applications and other areas.

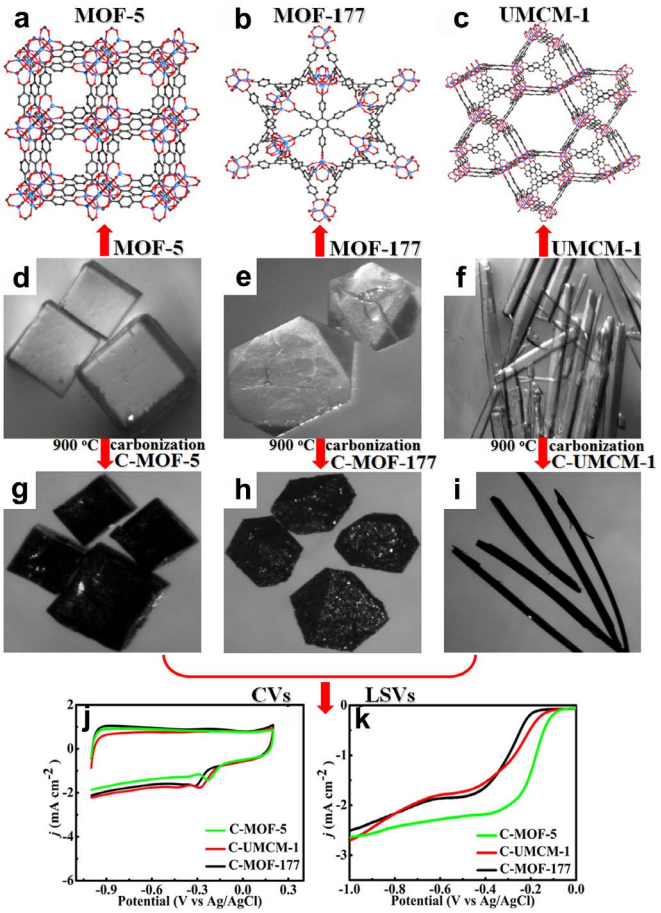

Figure 7 | (a–c) Structures, (d–i) Optical micrographs before and after carbonization, (j) CVs and (k) LSVs of different samples in O_2 saturated 0.1 M KOH solution.

Methods

Materials and preparation of the catalysts. All reagents were analytical grade and used without further purification. All solutions used in electrochemical experiments were prepared with Millipore water (≥18 MΩ).

In a typical procedure, 1 g MOFs were dried under vacuum at 60°C for 3 h and then soaked in a certain amount methanol solution in the presence of Dicyandiamide (DCDA), or DCDA and triphenylphosphane (TPP), or DCDA and dimethyl sulfoxide (DMSO), or DCDA, TPP and DMSO for about 12 h, respectively. The resulted MOFs were filtered and carbonized in a flow of ultrapure N_2 for 5 h at 900°C with the heating rate of 10°C min^{-1}. The obtained samples were collected and washed with dilute hydrochloric acid solution and distilled water. The doped products were dried under vacuum at 60°C for 5 h and denoted as N-C-MOF-5, NP-C-MOF-5, NS-C-MOF-5 and NPS-MOF-5, respectively. For comparison, the pristine MOF-5, UMCM-1 and MOF-177 were also treated under similar conditions (assigned as C-MOF-5, C-UMCM-1 and C-MOF-177), respectively.

Apparatus. The transmission electron microscopy (TEM) images were taken on a JEM-200CX instrument (Japan), using an accelerating voltage of 200 kV. The HRTEM images were recorded on JEOL-2100F apparatus at an accelerating voltage of 200 kV. Surface morphologies of the carbon materials were examined by a scanning electron microscope (SEM, JSM-7600F) at an acceleration voltage of 10 kV. The EDS spectra were taken on JSM-5160LV-Vantage typed energy spectrometer. The powder X-Ray diffraction (XRD) patterns were recorded on a D/max 2500 VL/PC diffractometer (Japan) equipped with graphite monochromatized Cu Kα radiation (λ = 1.54060 Å). Corresponding work voltage and current is 40 kV and 100 mA, respectively. X-ray photon spectroscopy (XPS) was recorded by a scanning X-ray microprobe (PHI 5000 Verasa, ULAC-PHI, Inc.) using Al kα radiation and the C1s peak at 284.6 eV as internal standard. The Raman spectra of dried samples were obtained on Lab-RAM HR800 with excitation by an argon ion laser (514.5 nm). The nitrogen adsorption-desorption experiments were operated at 77 K on a Micromeritics ASAP 2050 system. Prior to the measurement, the samples were degassed at 150°C for 10 h.

Electrodes preparation. All electrochemical experiments were conducted on a CHI 760D electrochemical station (Shanghai Chenhua Co., China) in a standard three electrode cell at room temperature. An Ag/AgCl with saturated KCl, and a Pt wire were used as reference and counter electrode, respectively.

The procedures of glass carbon electrodes (5.0 mm in diameter from Gamry Instruments, USA) preparation were as follows: prior to use, the electrodes were polished mechanically with aluminite power under an chamois, successively washed with ethanol and de-ionized water by sonication for 5 minutes, and dried in a desiccator. 4 mg of the catalysts were dispersed in 2 mL of solvent of Nafion (5%) and de-ionized water (1 : 9) by sonication, respectively. Typically, 10 μL (2 mg/mL) well-dispersed catalysts suspensions were pipetted onto the glassy carbon electrode surface and allowed to dry at room temperature for 30 minutes. For comparison, a commercially available Pt-C (20 wt%, Johnson Matthey) catalyst was prepared in the same way.

Electrocatalytic measurements. Cyclic voltammetry experiments (CVs) were performed at room temperature in 0.1 M KOH solutions which were purged with N_2 or O_2 for at least 30 minutes before measuring oxygen reduction reaction (ORR) activity from −1.0 to 0.2 V at a scan rate of 100 mV s^{-1}.

In the rotating disk electrode (RDE) test, the linear sweep voltammograms (LSVs) were measured in O_2 saturated 0.1 M KOH solution and the potential was varied from 0.2 to −1.0 V with a scan rate of 10 mV s^{-1} at various rotating speeds from 400 to 1600 rpm.

To examine the ORR performance, the number of electrons (n) was conducted according to Koutecky-Levich (K-L) equation:

$$J^{-1} = J_L{}^{-1} + J_k{}^{-1} = \left(B\omega^{1/2}\right)^{-1} + J_k{}^{-1} \quad (1)$$

$$B = 0.62nFC_{O2}(D_{O2})^{2/3}\nu^{-1/6} \quad (2)$$

$$J_k = nFkC_{O2} \quad (3)$$

Where J is the measured current density, J_k and J_L are the kinetic and diffusion-limiting current density, respectively. B is Levich slope which is given by (2). n is the number of electrons transferred for ORR. ω is the rotation rate (ω = 2 πN, N is the linear rotation speed), F is the Faraday constant (F = 96485 C mol^{-1}), ν is the kinetic viscosity, and C_{O2} is the concentration of O_2 ($1.2*10^{-3}$ mol L^{-1}), and D_{O2} is the diffusion coefficient of O_2 in 0.1 M KOH ($1.9*10^{-5}$ cm s^{-1}).

1. Bing, Y. H., Liu, H. S., Zhang, L., Ghosh, D. & Zhang, J. J. Nanostructured Pt-alloy electrocatalysts for PEM fuel cell oxygen reduction reaction. *Chem. Soc. Rev.* **39**, 2184–2202 (2010).
2. Debe, M. K. Electrocatalyst approaches and challenges for automotive fuel cells. *Nature* **486**, 43–51 (2012).
3. Nesselberger, M. *et al.* The effect of particle proximity on the oxygen reduction rate of size-selected platinum clusters. *Nat. Mater.* **12**, 919–924 (2013).
4. Anastasopoulos, A. *et al.* The Particle Size Dependence of the Oxygen Reduction Reaction for Carbon-Supported Platinum and Palladium. *ChemSusChem* **6**, 1973–1982 (2013).
5. Wu, J., Shi, M., Yin, X. & Yang, H. Enhanced Stability of (111)-Surface-Dominant Core–Shell Nanoparticle Catalysts Towards the Oxygen Reduction Reaction. *ChemSusChem* **6**, 1888–1892 (2013).
6. Zhao, X. *et al.* Recent advances in catalysts for direct methanol fuel cells. *Energy Environ. Sci.* **4**, 2736–2753 (2011).
7. Choi, S. I. *et al.* Synthesis and Characterization of 9 nm Pt-Ni Octahedra with a Record High Activity of 3.3 A/mg(Pt) for the Oxygen Reduction Reaction. *Nano Lett.* **13**, 3420–3425 (2013).
8. Cui, C. H., Gan, L., Heggen, M., Rudi, S. & Strasser, P. Compositional segregation in shaped Pt alloy nanoparticles and their structural behaviour during electrocatalysis. *Nat. Mater.* **12**, 765–771 (2013).
9. Wang, D. L. *et al.* Structurally ordered intermetallic platinum-cobalt core-shell nanoparticles with enhanced activity and stability as oxygen reduction electrocatalysts. *Nat. Mater.* **12**, 81–87 (2013).
10. Jang, J. H. *et al.* Rational syntheses of core-shell Fex@Pt nanoparticles for the study of electrocatalytic oxygen reduction reaction. *Sci. Rep.* **3**, 2872 (2013).
11. Wang, S. Y. *et al.* Vertically Aligned BCN Nanotubes as Efficient Metal-Free Electrocatalysts for the Oxygen Reduction Reaction: A Synergetic Effect by Co-Doping with Boron and Nitrogen. *Angew. Chem. Int. Ed.* **50**, 11756–11760 (2011).
12. Chen, S. *et al.* Nitrogen-Doped Carbon Nanocages as Efficient Metal-Free Electrocatalysts for Oxygen Reduction Reaction. *Adv. Mater.* **24**, 5593–5597 (2012).
13. Zhao, Y. *et al.* Can boron and nitrogen co-doping improve oxygen reduction reaction activity of carbon nanotubes? *J. Am. Chem. Soc.* **135**, 1201–1204 (2013).
14. Zheng, Y., Liu, J., Liang, J., Jaroniec, M. & Qiao, S. Z. Graphitic carbon nitride materials: controllable synthesis and applications in fuel cells and photocatalysis. *Energy Environ. Sci.* **5**, 6717–6731 (2012).
15. Xiong, W. *et al.* 3-D Carbon Nanotube Structures Used as High Performance Catalyst for Oxygen Reduction Reaction. *J. Am. Chem. Soc.* **132**, 15839–15841 (2010).
16. Liu, R., Wu, D., Feng, X. & Müllen, K. Nitrogen-doped ordered mesoporous graphitic arrays with high electrocatalytic activity for oxygen reduction. *Angew. Chem. Int. Ed.* **49**, 2565–2569 (2010).
17. Zheng, Y., Jiao, Y., Jaroniec, M., Jin, Y. & Qiao, S. Z. Nanostructured metal-free electrochemical catalysts for highly efficient oxygen reduction. *Small* **8**, 3550–3566 (2012).
18. Feng, L. Y. *et al.* Enhancing Electrocatalytic Oxygen Reduction on Nitrogen-Doped Graphene by Active Sites Implantation. *Sci. Rep.* **3**, 3306 (2013).
19. Pachfule, P., Dhavale, V. M., Kandambeth, S., Kurungot, S. & Banerjee, R. Porous-organic-framework-templated nitrogen-rich porous carbon as a more proficient electrocatalyst than Pt/C for the electrochemical reduction of oxygen. *Chem. Eur. J.* **19**, 974–980 (2013).
20. Liu, Z. W. *et al.* Phosphorus-doped graphite layers with high electrocatalytic activity for the O_2 reduction in an alkaline medium. *Angew. Chem. Int. Ed.* **50**, 3257–3261 (2011).
21. Yang, D. S., Bhattacharjya, D., Inamdar, S., Park, J. & Yu, J. S. Phosphorus-doped ordered mesoporous carbons with different lengths as efficient metal-free electrocatalysts for oxygen reduction reaction in alkaline media. *J. Am. Chem. Soc.* **134**, 16127–16130 (2012).
22. Zhang, C., Mahmood, N., Yin, H., Liu, F. & Hou, Y. Synthesis of Phosphorus-Doped Graphene and its Multifunctional Applications for Oxygen Reduction Reaction and Lithium Ion Batteries. *Adv. Mater.* **25**, 4932–4937 (2013).
23. Paraknowitsch, J. P. & Thomas, A. Doping carbons beyond nitrogen: an overview of advanced heteroatom doped carbons with boron, sulphur and phosphorus for energy applications. *Energy Environ. Sci.* **6**, 2839–2855 (2013).
24. Su, Y. *et al.* Low-temperature synthesis of nitrogen/sulfur co-doped three-dimensional graphene frameworks as efficient metal-free electrocatalyst for oxygen reduction reaction. *Carbon* **62**, 296–301 (2013).
25. Yang, Z. *et al.* Sulfur-Doped Graphene as an Efficient Metal-free Cathode Catalyst for Oxygen Reduction. *ACS nano* **6**, 205–211 (2012).
26. Liang, J., Jiao, Y., Jaroniec, M. & Qiao, S. Z. Sulfur and Nitrogen Dual-Doped Mesoporous Graphene Electrocatalyst for Oxygen Reduction with Synergistically Enhanced Performance. *Angew. Chem. Int. Ed.* **51**, 11496–11500 (2012).
27. Jeon, I. Y. *et al.* Large-scale production of edge-selectively functionalized graphene nanoplatelets via ball milling and their use as metal-free electrocatalysts for oxygen reduction reaction. *J. Am. Chem. Soc.* **135**, 1386–1393 (2013).
28. Yang, S. *et al.* Efficient Synthesis of Heteroatom (N or S)-Doped Graphene Based on Ultrathin Graphene Oxide-Porous Silica Sheets for Oxygen Reduction Reactions. *Adv. Func. Mater.* **22**, 3634–3640 (2012).
29. Long, J. R. & Yaghi, O. M. The pervasive chemistry of metal-organic frameworks. *Chem. Soc. Rev.* **38**, 1213–1214 (2009).
30. Jiang, H. L. & Xu, Q. Porous metal-organic frameworks as platforms for functional applications. *Chem. Commun.* **47**, 3351–3370 (2011).
31. Zhou, H. C., Long, J. R. & Yaghi, O. M. Introduction to Metal-Organic Frameworks. *Chem. Rev.* **112**, 673–674 (2012).
32. Liu, B., Shioyama, H., Akita, T. & Xu, Q. Metal-organic framework as a template for porous carbon synthesis. *J. Am. Chem. Soc.* **130**, 5390–5391 (2008).

33. Li, S.-L. & Xu, Q. Metal–organic frameworks as platforms for clean energy. *Energy Environ. Sci.* **6**, 1656–1683 (2013).
34. Song, L. F. *et al.* Mesoporous metal-organic frameworks: design and applications. *Energy Environ. Sci.* **5**, 7508–7520 (2012).
35. Ma, S., Goenaga, G. A., Call, A. V. & Liu, D. J. Cobalt imidazolate framework as precursor for oxygen reduction reaction electrocatalysts. *Chem. Eur. J.* **17**, 2063–2067 (2011).
36. Zhao, D. *et al.* Iron imidazolate framework as precursor for electrocatalysts in polymer electrolyte membrane fuel cells. *Chem. Sci.* **3**, 3200–3205 (2012).
37. Su, P. *et al.* Nitrogen-doped carbon nanotubes derived from Zn–Fe-ZIF nanospheres and their application as efficient oxygen reduction electrocatalysts with in situ generated iron species. *Chem. Sci.* **4**, 2941–2946 (2013).
38. Palaniselvam, T., Biswal, B. P., Banerjee, R. & Kurungot, S. Zeolitic Imidazolate Framework (ZIF)-Derived, Hollow-Core, Nitrogen-Doped Carbon Nanostructures for Oxygen-Reduction Reactions in PEFCs. *Chem. Eur. J.* **19**, 9335–9342 (2013).
39. Li, J. *et al.* Metal-organic framework templated nitrogen and sulfur co-doped porous carbons as highly efficient metal-free electrocatalysts for oxygen reduction reactions. *J. Mater. Chem. A* **2**, 6316–6319 (2014).
40. Choi, C. H., Chung, M. W., Park, S. H. & Woo, S. I. Additional doping of phosphorus and/or sulfur into nitrogen-doped carbon for efficient oxygen reduction reaction in acidic media. *Phys. Chem. Chem. Phys.* **15**, 1802–1805 (2013).
41. Choi, C. H., Park, S. H. & Woo, S. I. Binary and Ternary Doping of Nitrogen, Boron, and Phosphorus into Carbon for Enhancing Electrochemical Oxygen Reduction Activity. *ACS nano* **6**, 7084–7091 (2012).
42. Eddaoudi, M., Li, H. & Yaghi, O. M. Highly Porous and Stable Metal−Organic Frameworks: Structure Design and Sorption Properties. *J. Am. Chem. Soc.* **122**, 1391–1397 (2000).
43. Chen, P., Xiao, T.-Y., Qian, Y.-H., Li, S.-S. & Yu, S.-H. A nitrogen-doped graphene/carbon nanotube nanocomposite with synergistically enhanced electrochemical activity. *Adv. Mater.* **25**, 3192–3196 (2013).
44. Xu, J., Dong, G., Jin, C., Huang, M. & Guan, L. Sulfur and nitrogen co-doped, few-layered graphene oxide as a highly efficient electrocatalyst for the oxygen-reduction reaction. *ChemSusChem* **6**, 493–499 (2013).
45. Liu, B., Shioyama, H., Jiang, H., Zhang, X. & Xu, Q. Metal-organic framework (MOF) as a template for syntheses of nanoporous carbons as electrode materials for supercapacitor. *Carbon* **48**, 456–463 (2010).
46. Koh, K., Wong-Foy, A. G. & Matzger, A. J. A crystalline mesoporous coordination copolymer with high microporosity. *Angew. Chem. Int. Ed.* **47**, 677–680 (2008).

Acknowledgments

This work was financially supported by the NSFC (No. 21171096 and 21371099), the program of Jiangsu Specially-Appointed Professor, the project funded by the Priority Academic Program Development of Jiangsu Higher Education Institutions, the Foundation of Jiangsu Collaborative Innovation Center of Biomedical Functional Materials and University Postgraduate Research and Innovation Project in Jiangsu Province (CXLX13_368).

Author contributions

Y.L. and J.L. designed the experiments and wrote the main manuscript text, J.L., S.L., Y.T., K.L., L.Z. and N.K. performed experiments, J.B. and Z.D. provided sampels. All authors reviewed the manuscript.

Additional information

Supplementary information accompanies this paper at http://www.nature.com/scientificreports

Competing financial interests: The authors declare no competing financial interests.

How to cite this article: Li, J.-S. *et al.* Heteroatoms ternary-doped porous carbons derived from MOFs as metal-free electrocatalysts for oxygen reduction reaction. *Sci. Rep.* **4**, 5130; DOI:10.1038/srep05130 (2014).